Submitted to Metallurgical Transactions

LBL-2777
Preprint

GRAIN SIZE VERSUS DUCTILE-BRITTLE TRANSITION IN AN Fe-12% Ni ALLOY

Go Sasaki and Michael J. Yokota

July, 1974

Prepared for the U. S. Atomic Energy Commission
under Contract W-7405-ENG-48

TWO-WEEK LOAN COPY

This is a Library Circulating Copy which may be borrowed for two weeks. For a personal retention copy, call Tech. Info. Division, Ext. 5545

LAWRENCE BERKELEY LABORATORY • UNIVERSITY OF CALIFORNIA • BERKELEY

LBL-2777

DISCLAIMER

This document was prepared as an account of work sponsored by the United States Government. While this document is believed to contain correct information, neither the United States Government nor any agency thereof, nor the Regents of the University of California, nor any of their employees, makes any warranty, express or implied, or assumes any legal responsibility for the accuracy, completeness, or usefulness of any information, apparatus, product, or process disclosed, or represents that its use would not infringe privately owned rights. Reference herein to any specific commercial product, process, or service by its trade name, trademark, manufacturer, or otherwise, does not necessarily constitute or imply its endorsement, recommendation, or favoring by the United States Government or any agency thereof, or the Regents of the University of California. The views and opinions of authors expressed herein do not necessarily state or reflect those of the United States Government or any agency thereof or the Regents of the University of California.

GRAIN SIZE VERSUS DUCTILE-BRITTLE TRANSITION IN AN Fe-12% Ni ALLOY

Go Sasaki and Michael J. Yokota

Inorganic Materials Research Division, Lawrence Berkeley Laboratory and Department of Materials Science and Engineering, College of Engineering; University of California, Berkeley, California 94720

In a number of communications to this journal,[1-3] the question of a strong vs a weak dependence of the ductile-brittle transition temperature (DBTT) on grain size in iron and Fe-Ni alloys has been debated. Leslie, et al.[4] reasoned that removal of interstitial solutes by the addition of titanium to iron eliminated most of the grain size dependence of notch impact resistance, while Gupta and others[1,2] argued that a stronger relationship existed. But when Leslie[3] plotted the data available from the most recent studies, their slopes all fell within a narrow 6 to 7°K per $mm^{-1/2}$ range. We report here the grain size dependence of the ductile-brittle transition temperature for standard full size Charpy V-notch specimens of an Fe-12% Ni 0.3% Ti alloy. This alloy differs from the iron and Fe-low Ni alloys examined previously in that when it is quenched from the austenite phase a martensitic rather than a ferritic substructure is formed.

An example of the lath martensite structure typical of Fe-high Ni alloys is shown in Fig. 1a. The smaller areas within each prior austenite grain exhibiting different etching characteristics are lath packets, within which the martensite laths are arranged roughly parallel to each other. Figure 2 shows the laths to have widths that vary between 0.5 and 1.0 μm and to contain a dislocation, density of about 10^{11} to $10^{12}/cm^2$.

The austenite grain rather than the lath packet to describe the structure because the features of the brittle fracture surface for Fig. 1b suggested that it played the dominant role in imparting fracture resistance. It is apparent, for example, that the high-angle cleavage facets in Fig. 1b delineate the prior austenite grains. Alternatively, the lath packet size could have been used, for it follows a constant size relationship of 1 to 2.1 with the austenite grain for all the grain sizes studied (Fig. 3). Because of this constant size relationship, data plotted using either lath packet size or austenite grain size would result in the same grain size dependence of the DBTT.

Six different austenite grain sizes ranging from 4 to 50 μm were produced by quenching from various temperatures in the austenite phase field. In order to produce the smaller grain sizes the austenitizing and quenching steps were repeated a number of times. For the 3 larger grain sizes studied, the ductile-brittle transition temperatures based on the point of inflexion of the energy absorbtion curve fell on a slope of 6°C per $mm^{-1/2}$, Fig. 4, which is the same grain size dependence of notch toughness Leslie found for iron and Fe-low Ni alloys. The identical grain size dependence of the DBTT for two dissimilar substructures and different Ni contents indicates that Ni content and substructure morphology act as independent and constant factors determining the general level of fracture resistance within each alloy.

The ductile-brittle transition temperature deviates sharply from the initial slope, however, for the 3 smaller grain sizes studied. There is no significant difference in the microstructures between the

two groups of grain sizes, other than the gradual change of the substructure which tended more toward equiaxed ferrite as the grain size was decreased. This change, if significant, should actually raise rather than lower the DBTT, based on the observation of Yokota, et al.[6] and Roberts,[7] who found that equiaxed ferrite was less effective than lath martensite in lowering the DBTT.

Retained austenite was also ruled out as a factor, for no measurable amounts (<2%) of it were found. Increasing amounts of retained austenite are known to lower the DBTT[5] but at a rate of only a few degrees K° per volume percent of austenite. Other reasons for the sharp drop of the DBTT with smaller grain sizes can be postulated, particularly new modes of deformation promoted by low temperatures and ultrafine grain sizes, the cause for the apparent deviation of the grain size dependence lies more likely in adiabatic heating associated with very-low-temperature impact testing.

The changes in the engineering tensile stress-strain curves as a function of temperature are plotted in Fig. 5 for the microstructure shown in Fig. 1a. Smooth stress-strain curves were obtained down to liquid nitrogen temperature. However, serrated or jerky flow occurred at liquid helium temperature. Furthermore, serrated yielding at this temperature occured for all of the grain sizes examined.

This behavior suggests that serrated flow is associated more with the low testing temperature than with a-y particular microstructural feature. Basinski[8] found similar behavior at liquid He temperature for a number of alloys having a variety of microstructures and crystal structures. He attributed it to unstable flow produced by heat released

during deformation. The unstable flow is not observed at room temperature because the heat liberated is too small to produce any appreciable softening of the material. But because of the rapid decrease in the heat capacity at very low temperatures, this same heat can cause a much greater temperature rise at liquid He temperature. For bcc structures in particular, where the flow stress decreases sharply with increasing temperature, even a relatively small temperature rise can produce a large drop in the yield stress.

From Figs. 5 and 6 a rough estimate was made of the temperature rise during the liquid He tensile test by first determining the decrease (1.0×10^3 MN/m^2) in the stress level after the first serration (Fig. 5) and then noting the corresponding temperature which produces this level of yield stress, namely 50°K (Fig. 6). If similar heat generation can be assumed to occur in a Charpy V-notch specimen tested at liquid He temperature, the Charpy specimen should also experience an effective temperature of 50°K. When this correction is made for the Charpy tests conducted at liquid He for the three smaller grain sizes, their transition temperatures fall on the original $6°C/mm^{-1/2}$ slope established by the 3 large grain sizes (Fig. 4).

This result strongly suggests that heat generated by the deformation process is the cause for the sudden improvement in the notch impact resistance below liquid nitrogen testing temperatures and that much care should be exercised in the interpretation of impact test data below this temperature. Also significant is that the 6°C per $mm^{-1/2}$ grain size dependence on the DBTT holds for the interstitial-free bcc

Fe-Ni system, independent of the Ni content and the substructure (equiaxed ferrite vs lath martensite). Extrapolation of the data of Fig. 4 indicates that the 12% Ni alloy will not experience a ductile-brittle transition at liquid He temperature if its austenite grain size can be refined to 2 μm or the lath packet size to 1 μm, which is roughly the size of individual martensite laths.

ACKNOWLEDGEMENT

This work was done under the auspices of the U. S. Atomic Energy Commission.

REFERENCES

1. J. H. Bucher and R. H. Goodenow: Met. Trans., 1970, vol. 1, p. 2344.
2. Indra Gupta: Met. Trans., 1971, vol. 2, p. 323.
3. W. C. Leslie: Met. Trans., 1971, vol. 2, p. 1989.
4. W. C. Leslie, R. J. Sober, S. G. Babcock and S. J. Green: Trans. ASM, 1969, vol. 62, p. 690.
5. M. J. Schanfein, M. J. Yokota, V. F. Zackay, E. R. Parker and J. W. Morris, Jr.: The Cryogenic Properties of Fe-Mn and Fe-Mn-Cr Alloys presented at the ASTM Symposium on properties of Materials for LNG Tankage, May 21-22, 1974, Boston, Mass.
6. M. J. Yokota, V. F. Zackay and E. R. Parker: unpublished research. Inorganic Materials Research Division, Lawrence Berkeley Laboratory. Berkeley, California , 1974.
7. M. J. Roberts: Met. Trans., 1970, vol. 1, p. 3287.
8. Z. S. Basinski: Proc. Roy. Soc. (London) Series A, 1957, vol. 240, p. 299.

FIGURE CAPTIONS

Fig. 1. Fe-12% Ni-0.3% Ti austenitized at 900°C for 2 hr and water quenched: (a) light micrograph, (b) scanning electron micrograph of Charpy V-notch specimen broken at LN temperature.

Fig. 2. Transmission electron mictograph of lath martensite.

Fig. 3. Lath packet size vs austenite grain size.

Fig. 4. Ductile-brittle transition temperature vs austenite grain size.

Fig. 5. Engineering tensile stress vs strain at (a) room temperature, (b) methyl alcohol-dry ice, (c) liquid nitrogen, (d) liquid helium.

Fig. 6. Yield and ultimate tensile stress vs testing temperature.

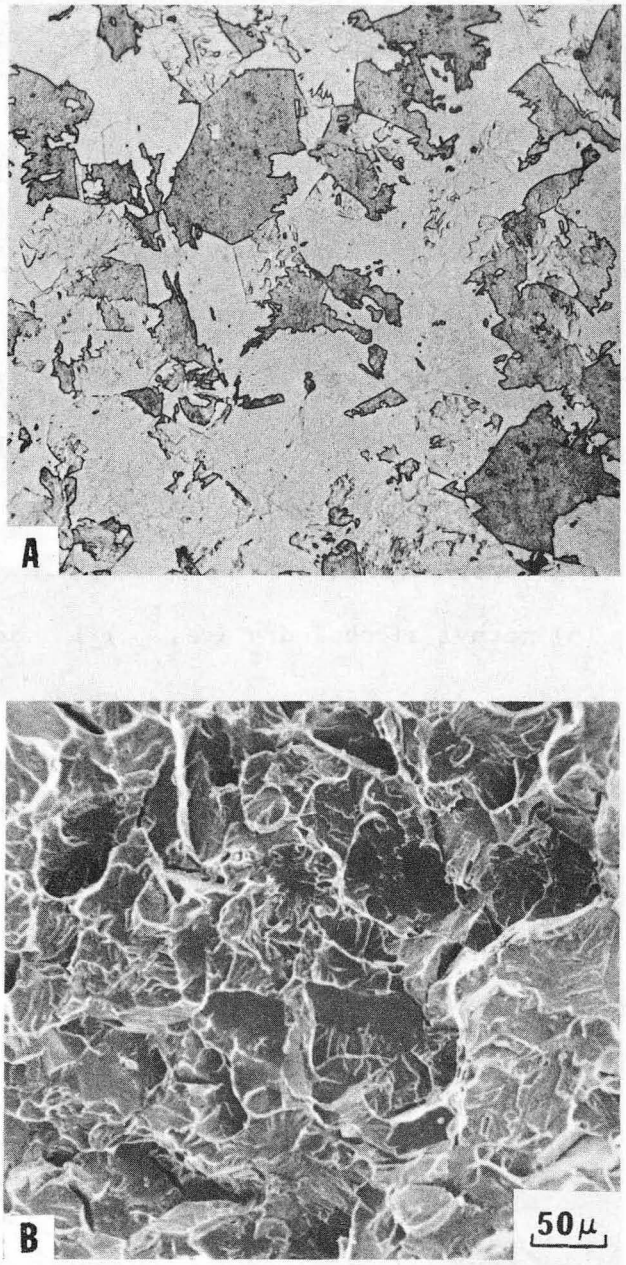

XBB 747-5412

Fig. 1

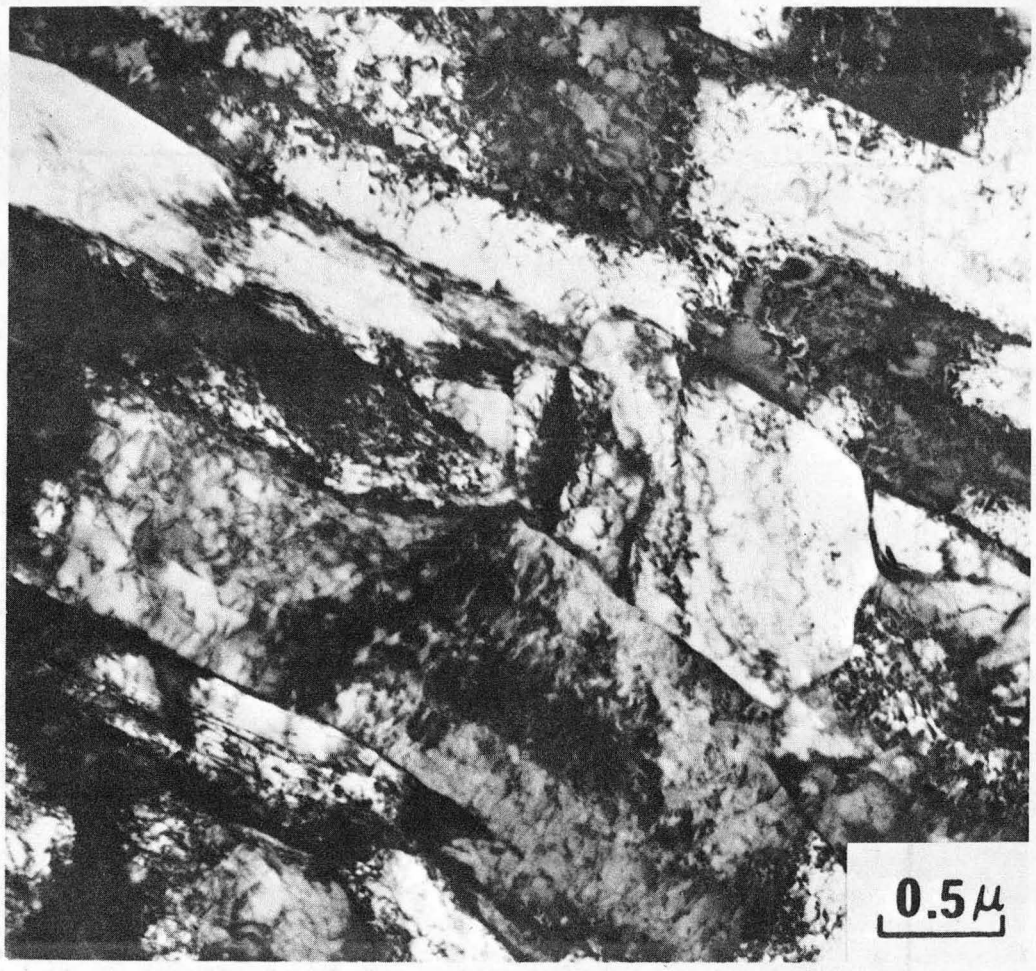

XBB 747-4850

Fig. 2

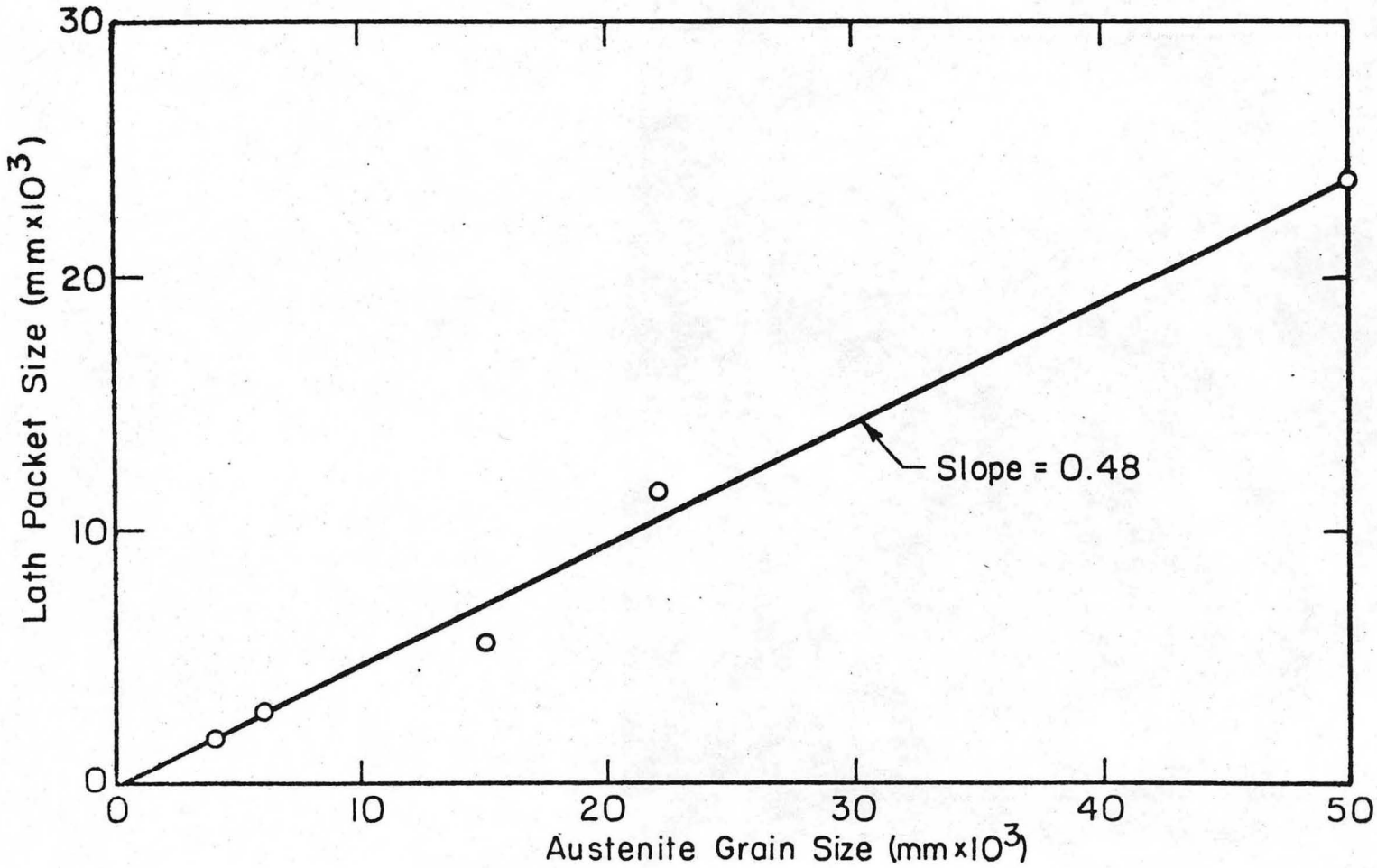

XBL 747-6663

Fig. 3

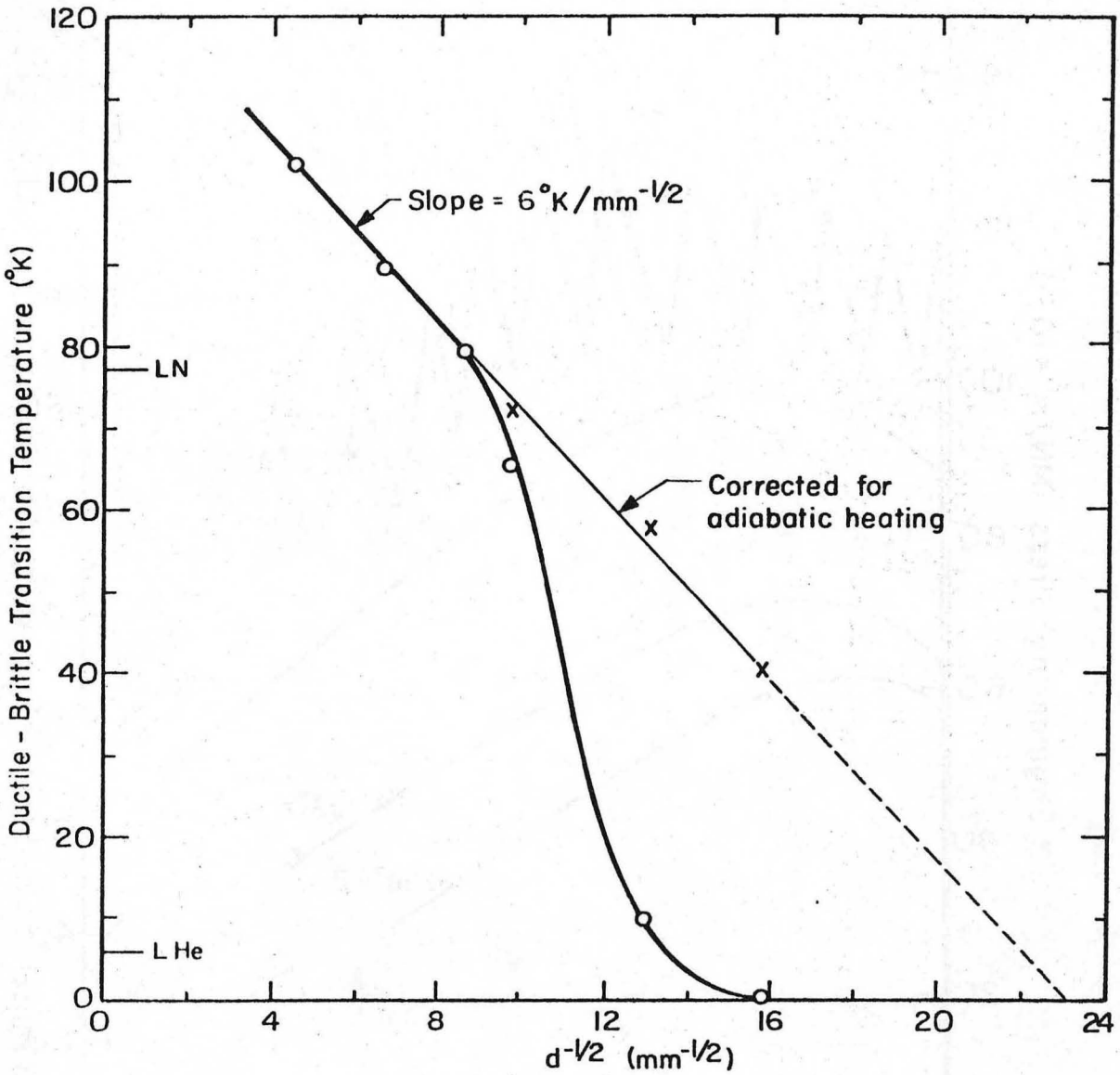

XBL 747-6664

Fig. 4

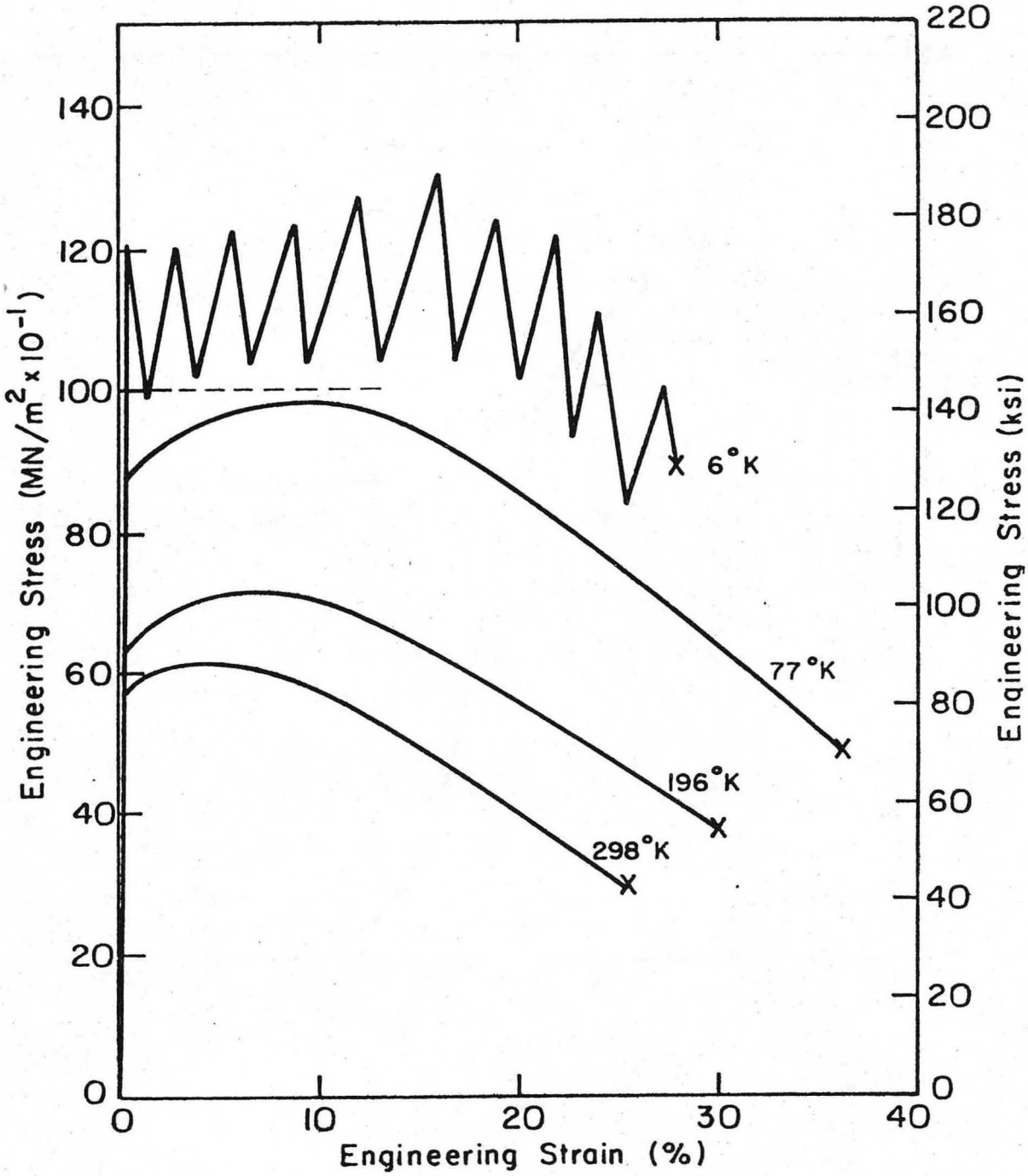

XBL 747-6665

Fig. 5

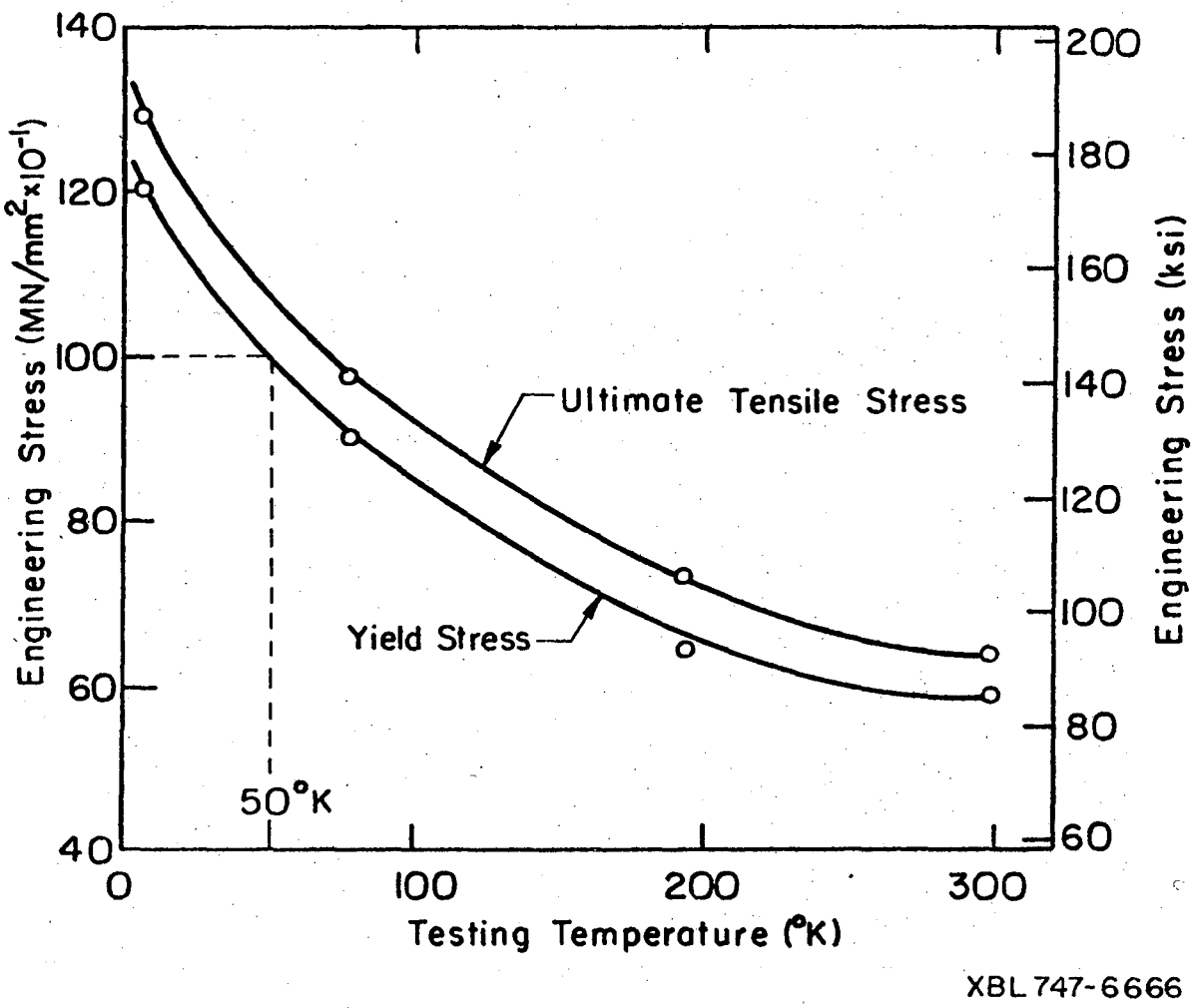
140
120
100
80
60
40
200
180
160
140
120
100
80
60
0
100
200
300
Engineering Stress (MN/mm²×10⁻¹)
Engineering Stress (ksi)
Testing Temperature (°K)
Ultimate Tensile Stress
Yield Stress
50°K
XBL 747-6666

Fig. 6

LEGAL NOTICE

This report was prepared as an account of work sponsored by the United States Government. Neither the United States nor the United States Atomic Energy Commission, nor any of their employees, nor any of their contractors, subcontractors, or their employees, makes any warranty, express or implied, or assumes any legal liability or responsibility for the accuracy, completeness or usefulness of any information, apparatus, product or process disclosed, or represents that its use would not infringe privately owned rights.

TECHNICAL INFORMATION DIVISION
LAWRENCE BERKELEY LABORATORY
UNIVERSITY OF CALIFORNIA
BERKELEY, CALIFORNIA 94720